Biosensors and Bioelectronics 55 (2014) 266–271

Contents lists available at ScienceDirect

Biosensors and Bioelectronics

journal homepage: www.elsevier.com/locate/bios

Dual amplified and ultrasensitive electrochemical detection of mutant DNA Biomarkers based on nuclease-assisted target recycling and rolling circle amplifications

Qiong Wang, Cuiyun Yang, Yun Xiang*, Ruo Yuan, Yaqin Chai

Key Laboratory on Luminescence and Real-Time Analysis, Ministry of Education, School of Chemistry and Chemical Engineering, Southwest University, Chongqing 400715, PR China

ARTICLE INFO

Article history:
Received 17 September 2013
Received in revised form
20 November 2013
Accepted 11 December 2013
Available online 21 December 2013

Keywords:
Electrochemical
Target recycling
Rolling circle amplification
G-quadruplex

ABSTRACT

Based on nicking endonuclease (NEase)-assisted target recycling and rolling circle amplification (RCA) for *in situ* generation of numerous G-quadruplex/hemin complexes, we developed a new, dual amplified and ultrasensitive electrochemical biosensor for mutant human p53 gene. The target mutant DNA hybridizes with the loop portion of a dithiol-modified hairpin probe (HP) self-assembled on a gold sensing electrode and forms nicking site for the NEase, which cleaves the HP and releases the target DNA. The released target DNA again hybridizes with the intact HP and initiates the DNA recycling process with the assistance of the NEase, leading to the cleavage of a large number of the HPs and the generation of numerous primers for RCA. With rationally designed, G-quadruplex complementary sequence-encoded RCA circular template, subsequent RCA results in the formation of long DNA sequences with massive tandem-repeat G-quadruplex sequences, which further associate with hemin and generate significantly amplified current response for highly sensitive DNA detection down to 0.25 fM. The developed method also exhibits high specificity for the target DNA against single-base mismatched sequence. With the ultrahigh sensitivity feature induced by the dual signal amplification, the proposed method can thus offer new opportunities for the detection of trace amounts of DNA.

1. Introduction

Sensitive and selective detection of sequence-specific DNA has become increasingly important in modern life sciences owing to its potential applicability ranging from genetic research of diseases to clinical diagnosis and therapy (Wang, 2000; Rosi and Mirkin, 2005; Li et al., 2010a). Over the past decades, various analytical protocols, including fluorescent (Zuo et al., 2010; Ryoo et al., 2012), electrochemical (EC) (Zhang et al., 2009; Wang et al., 2013), chemiluminescent (Liu et al., 2011) and colorimetric (Ji et al., 2011; Liu and Lu, 2006) approaches, have been implemented to achieve sensitive detection of DNA. Among these techniques, the EC approach as a promising tool for DNA detection has attracted particular attention in different fields owing to its inherent advantages such as simplicity, rapidness and low cost (Lei and Ju, 2012; Paleĉek and Bartoŝík, 2012). Despite the attractive progresses, the development of EC DNA sensors with ultrahigh sensitivity, selectivity and simplicity and the discrimination of single-base mismatch still remain major challenges.

In order to push down the detection limit, the development of effective signal amplification strategies for DNA detection continues to attract tremendous research interest (Comstock et al., 2011; Sorgenfrei et al., 2011). Although traditional polymerase chain reaction (PCR) (Heid et al., 1996) has been the most widely used method for DNA detection, it suffers the drawbacks of high cost, easy contamination and expert operation (Nallur et al., 2001; Giljohann and Mirkin, 2009). In recent years, various signal amplification strategies have been suggested to overcome the PCR-related shortcomings by using amplification labels such as enzymes (Patolsky et al., 2001; Gao et al., 2011), nanomaterials (Wang et al., 2003; Xu et al., 2009) and DNA biobarcode (Li et al., 2010b) or using the nuclease-assisted target recycling strategies. The target DNA recycling amplification methods via nuclease, such as polymerase-mediated isothermal strand displacement amplification (ISDA) (Guo et al., 2009; He et al., 2010), exonuclease III-aided signal amplification (Wu et al., 2011; Liu et al., 2013; Su et al., 2011) and nicking endonuclease signal amplification (NESA) (Xu et al., 2009; Chen et al., 2010; Ji et al., 2012), wherein a single target can be amplified to cyclically produce multiple hybridization events, have increasingly become attractive alternatives for the detection of trace levels of target DNA. NESA has received particular interest due to the distinct specificity for single-base

* Corresponding author. Tel.: +86 236 825 2277; fax: +86 236 825 4000.
E-mail address: yunatswu@swu.edu.cn (Y. Xiang).

0956-5663/$ - see front matter © 2013 Elsevier B.V. All rights reserved.
http://dx.doi.org/10.1016/j.bios.2013.12.034

mismatch detection capability and high sensitivity (Li et al., 2011; Xue et al., 2012a). In a typical NESA design, the target DNA hybridizes with a probe to create a nicking endonuclease (NEase) restriction site, which is recognized by sequence-specific NEase. After the NEase cleaves the probe in a DNA duplex into two pieces, the target DNA is released and then initiates next hybridization, cleavage, and dissociation process, which results in target recycling and signal amplification (Yin et al., 2012). Owing to the specific recognition of sequences, these NEase-assisted target recycling strategies obviate extra probe modification or conjugation steps and the addition of many exogenous reagents. Additionally, by taking the advantage of the NEase, reactions can be performed under an isothermal condition without using specialized instrumentation, which offers the NEase-assisted target recycling method with the potential to be widespread for routine analysis.

The discovery of the enzyme-assisted DNA recycling strategy can offer new amplification routes for highly sensitive DNA monitoring by integrating other signal enhancement approach to achieve dual or multiple amplifications within one assay protocol. Here, by coupling NEase-assisted target DNA recycling with rolling circle amplification (RCA), we developed a new hybrid signal amplification strategy for highly sensitive EC detection of the mutant human p53 gene cancer biomarker DNA. RCA, as an advanced DNA amplification technique alternative to PCR, can achieve significant signal amplification via the production of thousands of repeated sequences under mild reaction conditions and with speediness, high efficiency, and specificity (Liu et al., 1996; Ji et al., 2012). Due to the drastic signal amplification power, RCA has been widely employed in various sensing schemes for the analyses of proteins and nucleic acids (Hu and Zhang, 2010; Yan et al., 2012; Xue et al., 2012b). In our approach, the target mutant p53 genes hybridize with the hairpin DNA probes on the senor surface and create nicking sites for NEase to initiate the target DNA recycling amplification process to cleave numerous probes. The cleaved probes on the sensor surface are subject to *in situ* RCA to generate massive long DNA sequences with repeat G-quadruplex units, which associate with hemin to form G-quadruplex/hemin complexes. Direct electron transfer between hemin and the sensing electrode during the potential scan thus can offer amplified current response for highly sensitive detection of the mutant p53 gene.

2. Experimental

2.1. Materials and reagents

Hemin, dimethyl sulfoxide (DMSO), 6-mercaptohexanol (MCH) and tris(2-carboxyethy)phosphine hydrochloride (TCEP) were purchased from Sigma (St. Louis, MO, USA). A hemin stock solution (10 mM) was prepared in DMSO and stored in dark at −20 °C. Tris–HCl, 4-(2-hydroxyethyl) piperazine-1 ethanesulfonic acid sodium salt (HEPES), and dNTPs were obtained from Shanghai Sangon Biological Engineering Technology & Services Co., Ltd. (Shanghai, China). The NEase, N.BstNB I (an endonuclease that recognizes the specific nucleotide sequence of 5′-GAGTC-3′in a double-stranded DNA) and 10 × NE Buffer 3 (50 mM NaCl, 10 mM Tris–HCl, 10 mM $MgCl_2$ and 1 mM dithiothreitol (DTT), pH 7.9) were purchased from New England Biolabs (Ipswich, MA, USA). Phi29 DNA polymerase, T4 DNA ligase and 10 × T4 DNA ligase buffer were obtained from Fermentas (Lithuania).

All synthetic oligonucleotides with sequences listed below were ordered from Shanghai Sangon Biological Engineering Technology & Services Co., Ltd. (Shanghai, China).

Dithiol-modified hairpin capture probe (HP): 5′-SH–$(CH_2)_6$-TTTTTT*ACACAGTGTA***CTCACACGAATTCATCTGAC*GAGTC*TTC-C↓AGTGTGATGA*TACACTGTGT*TTTTTT-$(CH_2)_6$–SH-3′. The HP contains four functional regions: (1) the italic parts at the two ends represent the complementary sequences of the stem arm; (2) the bold part is complementary to the bold part of the padlock probe; (3) the underlined part is the complementary sequence to the mutant target DNA and (4) ***GAGTC*** is the recognition sequence of N.BstNB I, and the arrow indicates the nicking position.

Padlock probe: 5′-p **ATTCGTGTGAG**AAAACCCAACCCGCCCTACC-CAAAA **GGAAGACTCGTCAGATGA**-3′ (the bold portion matches the bold sequence of the hairpin probe; the underlined letters is completely complementary with the G-quadruplex sequence, and p in the padlock probe represents phosphate at the 5′ end).

Mutant human p53 gene target: 5′-TCATCACACTGGAAGACTC-3′;

Single-base mismatched sequence (sDNA): 5′-TCATCACACTG-GAAGAATC-3′;

Non-complementary sequence (nDNA):5′-GACGTCTGACTTCCTG-CGA-3′.

All other reagents were of analytical grade and used as received. Aqueous solutions were prepared using ultrapure water (specific resistance of 18 MΩ-cm).

2.2. Preparation of the HP-modified sensing electrode

The gold electrode (AuE, 3 mm in diameter) was cleaned by immersion in a freshly prepared piranha solution (a 3:1 v/v mixture of concentrated H_2SO_4 and 30% H_2O_2) for 30 min. After rinsing thoroughly with water, the electrode was polished with 0.3 and 0.05 μm aluminum slurry, followed by sequential sonication in distilled water, ethanol and distilled water for 5 min each to remove residual alumina powder. The well-polished electrode was then subjected to electrochemical pretreatment in 0.5 M H_2SO_4 with potential scanning from 0.2 to 1.6 V until remarkable voltammetric peaks were obtained. After being dried with nitrogen, the electrode should be immediately used for HP immobilization.

The above gold electrode was then incubated with 0.25 μM pretreated HP in a immobilization buffer solution (10 mM Tris–HCl, 10 mM TCEP, 0.1 M EDTA, 10 mM $MgCl_2$, pH 7.4) for 12 h at room temperature. $MgCl_2$ was added into the electrolyte to induce the formation of the hairpin structure of the HP, as reported by previous literatures (Gao et al., 1999; Chen et al., 2010). After that, the electrode was immersed in 1 mM MCH solution for 1 h to reduce nonspecific DNA adsorption and to optimize the orientation of the capture probes, followed by rinsing with ultrapure water.

2.3. Target hybridization and nicking enzyme-assisted target recycling

For target hybridization, the MCH/HP/AuE was incubated with 10 μL of 10 mM Tris–HCl solution (1 mM EDTA, 100 mM NaCl, pH 7.4) containing different concentrations of target DNA for 1 h at room temperature. After washing with Tris–HCl buffer, 10 μL of N. BstNB I enzyme (3 units μL^{-1}) in NEBuffer 3 was added and incubated at 55 °C. After 60 min of nicking, the electrodes were rinsed with NEBuffer 3 and dried under a stream of nitrogen gas.

2.4. RCA generation of G-quadruplex/hemin complexes

For subsequent RCA process, 10 μL of solution containing 1 × ligase buffer (40 mM Tris–HCl, 10 mM $MgCl_2$, 10 mM DTT, 0.5 mM ATP, pH 7.8), 50 nM padlock probe, 0.2 U T4 ligase was added onto the electrode surface for hybridization with the HP fragments produced in nicking enzyme-assisted target recycling and incubated at 37 °C for 1 h. The introduction of the T4 ligase links the 5′ and 3′ termini of the padlock probe together to form

a circular template. The excess circular template was removed by washing twice with ultrapure water. The RCA reaction was initiated by the addition of 0.2 U phi29 DNA polymerase and 1 mM dNTP in 10 μL of RCA reaction buffer (50 mM, Tris HCl buffer, 10 mM magnesium acetate, 33 mM potassium acetate, 1 mM DTT, and 0.1% Tween 20, pH 7.5) and proceeded for 1 h at 37 °C. After that, the resulting electrode was thoroughly rinsed and incubated with 0.2 mM freshly prepared hemin in 20 mM HEPES buffer (150 mM NaCl, 40 mM KCl, pH 7.2) for 30 min to allow the association of hemin with the RCA amplified G-quarduplex sequences.

2.5. EC Measurements

EC measurements were conducted on a CHI 621D EC analyzer (CH Instruments, Shanghai, China) with a conventional three-electrode system comprising a modified gold working electrode, a platinum wire auxiliary electrode, and a saturated calomel reference electrode (SCE). Cyclic voltammetry was performed in 0.1 M KCl solution containing 1 mM $Fe(CN)_6^{3-/4-}$ within the potential range from −0.3 V to 0.4 V under a scan rate of 100 mV s^{-1}. Differential pulse voltammetry (DPV) was performed in the working solution (20 mM HEPES, 20 mM KCl, pH 8.0) between the potential range from −0.15 to −0.5 V with pulse amplitude of 50 mV and sample width of 16.7 ms. Before the measurements, the working solution was thoroughly purged with high purity nitrogen for 30 min to avoid the interference from the reduction of oxygen.

3. Results and discussion

3.1. Design principle of the dual amplified EC DNA biosensor

Our new dual amplified strategy for ultrasensitive mutant DNA detection is primarily based on a hybrid, significant signal enhancement approach by the coupling of NEase-assisted target recycling with RCA, which results in the formation of numerous G-quadruplex/hemin complexes on the sensor surface for the generation of amplified current signal output. In our experimental design, the dithiol-modified HPs, which contain four domains, the RCA primer region, the target mutant DNA recognition sequences, the NEase recognition sequences and two complementary sequences in the duplex structure of the stem, are employed as the probes. The NEase used here is N.BstNB I, which recognizes and cleaves only one strand of a double stranded DNA four bases away from the 3′end of its recognition sequence (5′-GAGTC-3′) (Chen et al., 2010). Scheme 1 depicts the principle of our mutant DNA detection protocol. The HPs are first self-assembled on the AuE through the Au–S bond, and this is followed by surface blocking with MCH to form a mixed monolayer (MCH/HP/AuE). Upon the addition of the target mutant p53 genes, they hybridize with the loop part of HPs to form double-stranded structures with full recognition sites for N.BstNB I, which preferentially binds to the recognition sites and selectively cleaves the HPs into two pieces, leaving the RCA primer sequence regions of the HPs available for subsequent RCA reactions. At the same time, upon N.BstNB I cleavage, the target genes dissociate from the HPs and again hybridize with the un-nicked HPs to initiate the target gene recycling process, which leads to permanent transformation of a large number of HPs to numerous RCA primer fragments. After incubating the resulting sensor surface with the rationally designed padlock probes and T4 ligase, the RCA reactions are initiated by adding phi29 DNA polymerase and dNTPs and massive long DNA molecules with multiple G-quadruplex units are therefore generated. These G-quadruplex units associate with hemin to form G-quadruplex/hemin complexes on the sensor surface with the help of K^+ (Zhang et al., 2010; Yang et al., 2012; Liu et al., 2013). During the potential scan, the bound hemin generates the current response for indirect EC detection of the mutant p53 gene (Yang et al., 2012; Jiang et al., 2013). Because of the hybrid signal amplification, the detection of trace amounts of the mutant p53 gene can thus be expected.

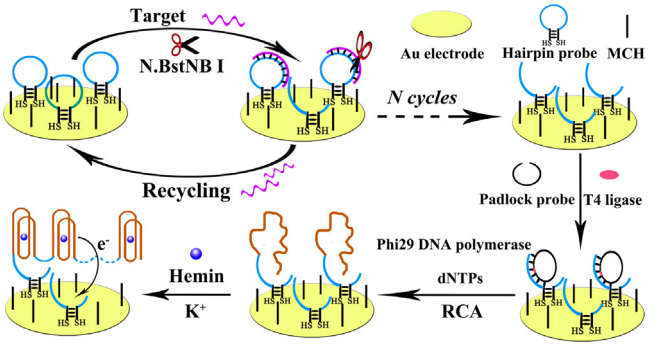

Scheme 1. Illustration of the dual amplified assay protocol for ultrasensitive EC detection of mutant DNA based on NEase-assisted target recycling and RCA hybrid signal amplification.

3.2. EC Characterizations of the biosensor

In order to follow the step-by-step construction of the sensor, the CV behavior of the electroactive species, $Fe(CN)_6^{3-/4-}$, was investigated at different stages of the sensor preparation. As shown in Fig. 1, the bare AuE exhibits a couple of quasi-reversible, well-defined redox peaks of $[Fe(CN)_6]^{3-/4-}$ (curve a). However, after the immobilization of the HPs and blocking with MCH on the electrode surface, significant decreases in redox currents and an increase in peak separation are observed (curve b), which is primarily ascribed to the electrostatic repulsion of the negatively charged $[Fe(CN)_6]^{3-/4-}$ from approaching the electrode surface by the negatively charged phosphate skeletons of DNA probes (Patolsky et al., 1999; Zhou et al., 2012), suggesting the successful formation of the self-assembled mix monolayer on the sensing surface. The redox current responses decreased further after being hybridized with the target DNA (curve c). As expected, the current responses are higly reduced while the peak separation is significantly increased (curve d) after the HP-modified AuE is further treated with N.BstNB I and subject to subsequent RCA reaction in the presence of the target DNA, due to the introduction of more negative charges on the AuE surface upon formation of the long DNA sequences.

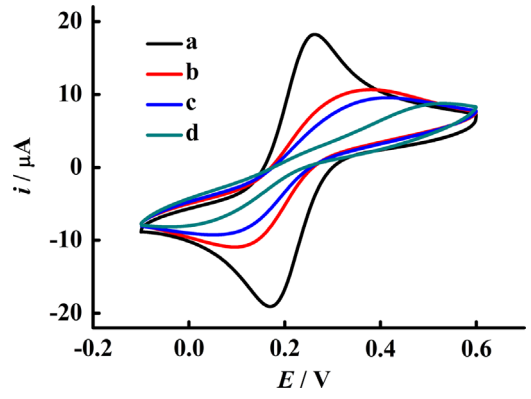

Fig. 1. Cyclic voltammograms for the AuE at different modification stages in 0.1 M KCl containing 1 mM $[Fe(CN)_6]^{3-/4-}$ by scanning the potential from –0.1 to 0.6 V at a scan rate of 50 mV s^{-1}: (a) bare AuE, (b) MCH/HP/AuE, (c) Target/MCH/HP/AuE, and (d) RCA/NEase/Target/MCH/HP/AuE.

3.3. Proof-of-concept detection of mutant DNA with the dual amplified method

To further verify the feasibility of the proposed method for the detection of the mutant DNA target, DPV measurements were performed on the sensing MCH/HP/AuE in the presence/absence of 30 U N.BstNB I with/without subsequent RCA reaction, followed by the incubation with 0.2 mM hemin. As shown in Fig. 2, when the MCH/HP/AuE sensors were incubated without (blank, curve a) and with (curve c) the mutant target DNA (5.0 pM, without RCA) with the presence of 30 U N.BstNB I, respectively, no apparent current responses were observed. When the N.BstNB I is removed from the sensing system, the presence of the mutant target DNA (5.0 pM) followed by RCA shows a negligible increase (curve b) compared with that of the blank test. These highly minimized current responses are basically due to the suppression of the formation of the G-quadruplex sequences either with the absence of the mutant target DNA (curve a) or the lack of RCA reaction (curve c)/ N.BstNB I (curve b) even with the presence of the target DNA. However, when the MCH/HP/AuE is incubated with the mutant target DNA and N.BstNB I, which is followed by the RCA reaction, a significantly amplified current response at around −0.35 V is observed (curve d). Such current response can be assigned to EC reduction of hemin incorporated into the G-quadruplex structures (Yang et al., 2012; Liu et al., 2013; Liu et al., 2013). This preliminary result for amplified detection of the mutant DNA indicates that the proposed method can be potentially employed to detect trace amounts of the mutant target DNA.

3.4. Optimizations for the assay conditions

To achieve optimal sensing performance, experimental parameters including RCA duration time and the concentration of hemin were investigated. The peak current responses at −0.35 V were selected to evaluate the performance of the proposed method. Fig. 3A depicts the effect of the RCA reaction time on the EC current response in the presence of the target mutant DNA (1 pM) and N.BstNB I (30 U). As anticipated, the peak current increases rapidly with the augment of the RCA reaction duration, and then reaches the maximum value at 60 min, which is due to the fact that with longer RCA reaction time, more copies of G-quandruplex complexes and longer DNA sequences are synthesized. However, longer RCA reaction time also increases the chance of inter- or intra-molecular misfolding or tangling of the long DNA products, especially due to the many G-rich segments located in the sequences (Tian et al., 2006; Tang et al., 2012). Afterward, the peak current decreases slightly possibly because of the entanglement of RCA products with each other (Ji et al., 2012; Su et al., 2010), which hinders hemin from accessing the G-quandruplex complexes. According to the results, either a longer or a shorter duration compromises the signal current output. Thus, 60 min is selected as the optimum reaction duration for RCA.

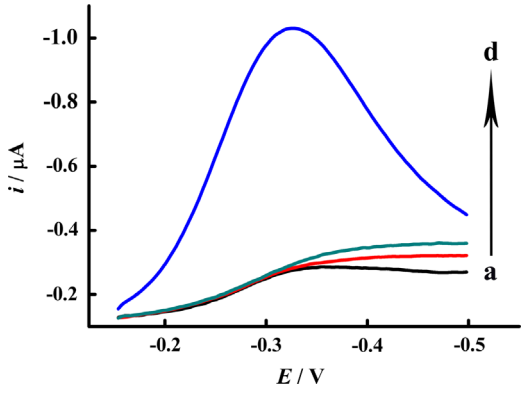

Fig. 2. Typical DPV responses of the sensing electrode incubated with (a) N.BstNB I (30 U); (b) the mutant target DNA (5 pM); (d) N.BstNB I (30 U) and mutant target DNA (5 pM) followed by RCA reaction for 60 min and (c) N.BstNB I (30 U) and the mutant target DNA (5 pM) without RCA.

Considering the important role of hemin in the formation of G-quadruplex/hemin complex and direct electron transfer of hemin, we also investigated the effect of the concentration of hemin on the current response. Fig. 3B displays the effect of different concentrations of hemin on the DPV peak current ratio (i/i_0), where, i_0 and i correspond to the current responses of the sensor with the absence and presence of the target gene, respectively. From Fig. 3B, we can see that the signal to noise ratio (i/i_0) increases gradually with increasing concentration of hemin, indicating that more hemin are intercalated into the G-quadruplex sequences after RCA. Correspondingly, numerous G-quadruplex/ hemin complexes are obtained and the current response of the sensing system is greatly enhanced. However, it should be noted that when the concentration of hemin is higher than 0.2 mM, the background signal from hemin itself is increased, leading to decreased DPV peak current ratio. Thus, the results indicated that the optimum concentration of hemin is 0.2 mM.

3.5. Sensitivity and selectivity of the EC biosensor

Under the above optimal experimental conditions, we examined the sensitivity of the proposed method upon the addition of different concentrations of the target mutant DNA. From the results shown in Fig. 4A, the elevated concentration of the target mutant DNA from 1 fM to 100 pM causes a gradual increase in the current response. Fig. 4B outlines the calibration curve for quantitative analysis of target DNA, in which the current response of hemin shows a strong linear dependence upon the logarithm of the concentration of the target DNA over the range from 1 fM to 10 pM. The regression equation is i (μA) = −3.0135 − 0.1753 log c (i is the peak current and c is the concentration of the target DNA), with a correlation coefficient (R^2) of 0.9883, and the detection limit is calculated to be 0.25 fM based on a 3σ/slope rule (where σ is the relative standard deviation of the blank solutions, $n=11$). Such low detection limit of the proposed method lies in the hybrid signal amplification effect from the specific NEase-assisted target recycling and isothermal exponential RCA for *in situ* generation of numerous G-quadruplex/hemin complexes. The reproducibility of the proposed sensor were examined with six repeated experiments for the target DNA at 500 fM, and a relative standard deviation of 10.4% of the current responses was obtained, which suggested a good reproducibility of the method.

The specificity of the DNA sensor system was evaluated by using three different kinds of control DNA sequences, including the perfectly complementary sequence, the single-base mismatched sequence (sDNA) and the non-complementary sequence (nDNA), respectively. As shown in Fig. 5A, the presence of even 10-fold excess of the nDNA (5 pM, column b) and sDNA (5 pM, column c) causes minimal current responses, which are closed to that of the blank test. However, the presence of the perfectly matched target DNA at an even lower concentration (10-fold, 500 fM) results in a significant increase in the current response. These comparisons demonstrate that only the perfectly matched sequence can initiate the N.BstNB I-assisted target recycling and thus activate the RCA reaction to synthesize a large amount of the G-quadruplex/hemin complexes, which might be attributed to the high hybridization specificity of hairpin probe and target DNA and the high fidelity of nicking endonuclease (Chen et al., 2010; Ji et al., 2012). To investigate the validity of the proposed signal amplification strategy to real clinical samples, we challenged our sensing strategy with the presence of the target DNA in a complex sample matrix, 10% human serum (diluted with buffer). As shown in Fig. 5B, the DPV response obtained from

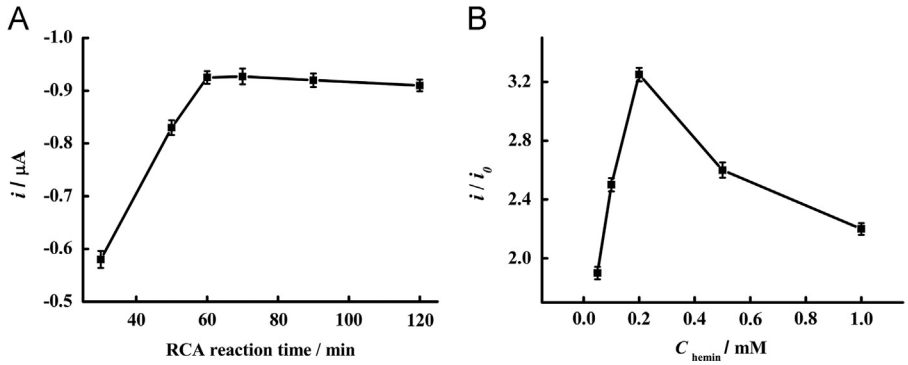

Fig. 3. The optimization of (A) RCA reaction time from 30 to 120 min and (B) the concentration of hemin from 0.05 to 1.0 mM for the proposed method with the presence of the target mutant DNA gene (1 pM) and N.BstNB I (30 U). Error bars: SD, $n=3$.

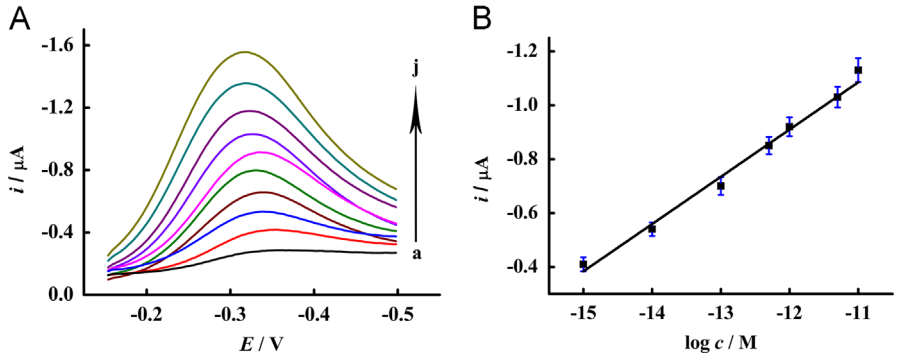

Fig. 4. (A) Typical DPV curves for analyzing different concentrations of target mutant DNA: (a) blank (0 fM), (b) 1 fM, (c) 10 fM, (d) 100 fM, (e) 500 fM, (f) 1 pM, (g) 5 pM, (h) 10 pM, (i) 50 pM and (j) 100 pM. (B) The corresponding calibration curve of log c *vs* DPV peak current response of hemin for the concentration of the target DNA from 1 fM to 10 pM. Error bars: SD, $n=3$.

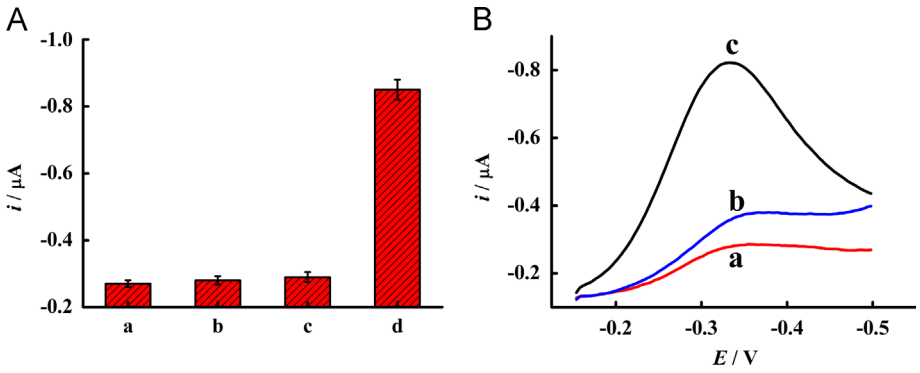

Fig. 5. (A) Specificity investigation of the proposed method for target DNA against nDNA and sDNA sequences: (a) blank, (b) nDNA (5 pM), (c) sDNA (5 pM), and (d) target DNA (500 fM). (B) DPV responses of the sensor for (a) blank, (b) 10% human serum only and (c) 500 fM of the target DNA in 10% human serum. Other conditions, as in Fig. 4.

the blank serum sample (in the absence of the spiked target DNA, curve b) shows slight increase compared with that of the blank test (curve a), which is presumably due to the sample matrix effect. When the serum sample was spiked with 500 fM target DNA, an obviously amplified current response (curve c) is observed, which indicates that our method can be applied to complex serum media.

4. Conclusions

In summary, by taking the advantage of the hybrid NEase-assisted target recycling and RCA for *in situ* production of massive G-quadruplex/hemin complexes, we have demonstrated a new ultrasensitive EC method for the detection of the mutant human p53 gene. The first amplification of our strategy is initiated by the NEase-assisted target recycling that the N.BstNB I recognizes the specific nicking sequences and cleaves the HPs upon hybridization with the target. Due to the recycling and reuse of the target DNA, the amount of the cleaved HP fragments can be dramatically increased, producing more RCA primers for triggering the post-amplification. With the rationally designed padlock DNA as circular templates, the resulting RCA products contains numerous, tandem-repeat G-quadruplex sequences for the association of a large number of hemin, which generates significantly amplified current response for the detection of the mutant human p53 gene down to 0.25 fM. The proposed method can also discriminate signal-base mismatched DNA from the target DNA. Although we only demonstrated the detection of the mutant human p53 gene

here, the proposed method can be extended for the detection of trace amounts of other DNA sequences with the selection of different endonucleases and carefully designed probe sequences.

Acknowledgments

This work was supported by National Nature Science Foundation of China (No. 21275004, 20905062, 21075100 and 21275119), the New Century Excellent Talent Program of MOE (NCET-12-0932), Fundamental Research Funds for the Central Universities (XDJK2012A004).

References

Chen, J.H., Zhang, J., Li, J., Fu, F.F., Yang, H.H., Chen, G.N., 2010. Chem. Commun. 46, 5939–5941.
Comstock, M.J., Ha, T., Chemla, Y.R., 2011. Nat. Methods 8, 335–340.
Gao, W.C., Dong, H.F., Lei, J.P., Ji, H.X., Ju, H.X., 2011. Chem. Commun. 47, 5220–5222.
Gao, Y., Robinson, H., Sanishvili, R., Joachimiak, A., Wang, A.H.J., 1999. Biochemistry 38, 16452–16460.
Giljohann, D.A., Mirkin, C.A., 2009. Nature 462, 461–464.
Guo, Q.P., Yang, X.H., Wang, K.M., Tan, W.H., Li, W., Tang, H.X., Li, H.M., 2009. Nucleic Acids Res. 37, e20.
He, Y.Q., Zeng, K., Zhang, X.B., Gurung, A.S., Balod, M., Xu, H., Liu, G.D., 2010. Electrochem. Commun. 12, 985–988.
Heid, C.A., Stevens, J., Livak, K.J., Williams, P.M., 1996. Genome Res. 6, 986–994.
Hu, J., Zhang, C.Y., 2010. Anal. Chem. 82, 8991–8997.
Ji, H.X., Dong, H.F., Yan, F., Lei, J.P., Ding, L., Gao, W.C., Ju, H.X., 2011. Chem. – Eur. J. 17, 11344–11349.
Ji, H.X., Yan, F., Lei, J.P., Ju, H.X., 2012. Anal. Chem. 84, 7166–7171.
Jiang, B.Y., Wang, M., Li, C., Xie, J.Q., 2013. Biosens. Bioelectron. 43, 289–292.
Lei, J.P., Ju, H.X., 2012. Chem. Soc. Rev. 41, 2122–2134.
Li, D., Song, S.P., Fan, C.H., 2010a. Acc. Chem. Res. 43, 631–641.
Li, H., Sun, Z., Zhong, W., Hao, N., Xu, D., Chen, H.Y., 2010b. Anal. Chem. 82, 5477–5483.
Li, J., Yao, Q.H., Fu, H.E., Zhang, X.L., Yang, H.H., 2011. Talanta 85, 91–96.
Liu, D.Y., Daubendiek, S.L., Zillman, M.A., Ryan, K., Kool, E.T., 1996. J. Am. Chem. Soc. 118, 1587–1594.
Liu, J.W., Lu, Y., 2006. Angew. Chem. Int. Ed. 45, 90–93.
Liu, S.F., Wang, C.F., Zhang, C.X., Wang, Y., Tang, B., 2013. Anal. Chem. 85, 2282–2288.
Liu, X.Q., Freeman, R., Golub, E., Willner, I., 2011. ACS Nano 5, 7648–7655.
Nallur, G., Luo, C.H., Fang, L.H., Cooley, S., Dave, V., Lambert, J., Kukanskis, K., Kingsmore, S., Lasken, R., Schweitzer, B., 2001. Nucleic Acids Res. 29, e118.
Paleček, E., Bartošík, M., 2012. Chem. Rev. 112, 3427–3481.
Patolsky, F., Katz, E., Bardea, A., Willner, I., 1999. Langmuir 15, 3703–3706.
Patolsky, F., Lichtenstein, A., Willner, I., 2001. Nat. Biotechnol. 19, 253–257.
Rosi, N.L., Mirkin, C.A., 2005. Chem. Rev. 105, 1547–1562.
Ryoo, S.R., Jang, H., Kim, K.S., Lee, B., Kim, K.B., Kim, Y.K., Yeo, W.S., Lee, Y., Kim, D.E., Min, D.H., 2012. Biomaterials 33, 2754–2761.
Sorgenfrei, S., Chiu, C.Y., Gonzalez, R.L., Jr, Yu, Y.J., Kim, P., Nuckolls, C., Shepard, K.L., 2011. Nat. Nanotechnol. 6, 126–132.
Su, J., Zhang, H.J., Jiang, B.Y., Zheng, H.Z., Chai, Y.Q., Yuan, R., Xiang, Y., 2011. Biosens. Bioelectron. 29, 184–188.
Su, Q., Xing, D., Zhou, X.M., 2010. Biosens. Bioelectron. 25, 1615–1621.
Tang, L.H., Liu, Y., Ali, M.M., Kang, D.K., Zhao, W.A., Li, J.H., 2012. Anal. Chem. 84, 4711–4717.
Tian, Y., He, Y., Mao, C.D., 2006. ChemBioChem 7, 1862–1864.
Wang, J., 2000. Nucleic Acids Res. 28, 3011–3016.
Wang, J., Liu, G.D., A, Merkoc i, 2003. J. Am. Chem. Soc. 125, 3214–3215.
Wang, Q.B., Lei, J.P., Deng, S.Y., Zhang, L., Ju, H.X., 2013. Chem. Commun. 49, 916–918.
Wu, D., Yin, B.C., Ye, B.C., 2011. Biosens. Bioelectron. 28, 232–238.
Xu, W., Xue, X.J., Li, T.H., Zeng, H.W., Liu, X.G., 2009. Angew. Chem. Int. Ed. 48, 6849–6852.
Xue, L.Y., Zhou, X.M., Xing, D., 2012a. Anal. Chem. 84, 3507–3513.
Xue, Q.W., Wang, Z.G., Wang, L., Jiang, W., 2012b. Bioconjug. Chem. 23, 734–739.
Yan, J., Su, S., He, S.J., He, Y., Zhao, B., Wang, D.F., Zhang, H.L., Huang, Q., Song, S.P., Fan, C.H., 2012. Anal. Chem. 84, 9139–9145.
Yang, N.N., Cao, Y., Han, P., Zhu, X.J., Sun, L.Z., Li, G.X., 2012. Anal. Chem. 84, 2492–2497.
Yin, B.C., Liu, Y.Q., Ye, B.C., 2012. J. Am. Chem. Soc. 134, 5064–5067.
Zhang, K., Zhu, X.L., Wang, J., Xu, L.L., Li, G.X., 2010. Anal. Chem. 82, 3207–3211.
Zhang, X.L., Li, L.L., Li, L., Chen, J., Zou, G.Z., Si, Z.K., Jin, W.R., 2009. Anal. Chem. 81, 1826–1832.
Zhou, Y.L., Wang, M., Meng, X.M., Yin, H.S., Ai, S.Y., 2012. RSC Adv. 2, 7140–7145.
Zuo, X.L., Xia, F., Xiao, Y., Plaxco, K.W., 2010. J. Am. Chem. Soc. 132, 1816–1818.